

Hybrid 2D Material Nanophotonics: A Scalable Platform for Low-Power Nonlinear and Quantum Optics

Arka Majumdar,^{*,†,‡} Christopher M. Dodson,[†] Taylor K. Fryett,[†] Alan Zhan,[‡] Sonia Buckley,[§] and Dario Gerace^{||}

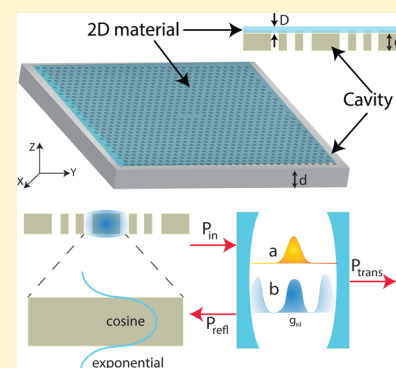
[†]Electrical Engineering and [‡]Physics Department, University of Washington, Seattle, Washington 98195, United States

[§]Department of Applied Physics, Stanford University, Stanford, California 94305, United States

^{||}Department of Physics, University of Pavia, Via Bassi 6, I-27100 Pavia, Italy

ABSTRACT: Two-dimensional, atomically thin materials offer unique physical properties, such as a large second-order optical nonlinearity. Integrating these materials into a scalable and silicon-compatible platform could provide a pathway toward realizing low-power nonlinear optics. We have presented a formalism to calculate the effective nonlinear optical coefficient for a cavity integrated 2D material system as well as the cavity enhanced absorptive loss, which can be used to guide future experiments. We have also shown that the few-photon regime of cavity QED is within reach with a cavity quality factor of $\sim 10^5$ – 10^6 , provided the loss at the second harmonic mode is minimized. As test applications, we have simulated the performances of (a) an optically bistable device and (b) a nanostructured device exhibiting single-photon blockade.

KEYWORDS: nonlinear optics, monolayer material, nanocavity, second order nonlinearity



Realizing nonlinear photon–photon interactions in a low power and scalable platform is important for both fundamental sciences as well as optical computing-based technologies, for example, exploring the utility of coherence in optical computing¹ or realizing quantum simulation using interacting photonic systems.^{2,3} Unfortunately, direct photon–photon coupling is weak, so any such coupling must be enhanced through an interaction with material excitations. In fact, such light–matter interactions can be enhanced by spatial and temporal confinement of light by using a nanophotonic cavity in combination with a strongly nonlinear material. However, for practical applications, there must also be a scalable fabrication process for the cavity-material system. Overcoming these limitations on scalability and low-power operation would help facilitate advances in optical computing as well as expand our understanding of fundamental quantum properties.

Unfortunately, these two requirements of scalability and strong nonlinearity are often contradictory for available solid-state material systems. For example, single photon nonlinearity can be readily achieved using single quantum emitters, for example, quantum dots or defect centers.^{4–7} Although this is indeed the strongest optical nonlinearity that can be achieved in solid-state quantum optics, the scalability of these emitters is limited due to their spatial and spectral inhomogeneity. Strongly nonlinear materials that could be selectively grown or easily positioned at a specific location would allow a more scalable fabrication process. Among the alternatives, semiconductor quantum wells possess a stronger nonlinearity than

bulk materials, which has led to the demonstrations of quantum simulators^{8,9} and optical switching devices¹⁰ using quantum wells coupled to distributed Bragg reflectors with moderate mode volume. Unfortunately, further enhancement of the nonlinear effect using smaller mode-volume cavities is difficult in these geometries due to an increase in surface roughness and electronic surface states during the etching process. Another candidate would be a bulk material possessing $\chi^{(2)}$ nonlinearity, like gallium arsenide (GaAs) or gallium phosphide (GaP), or a $\chi^{(3)}$ nonlinearity, like silicon (Si). However, owing to the weak nonlinear nature of bulk susceptibilities, we would need an ultrahigh quality (Q) factor to reach an appreciable nonlinearity at the single-photon level, as recently pointed out.^{11,12}

Two-dimensional (2D) materials are single atomic monolayers of material, which can be metallic, semiconducting, or insulating.¹³ They exhibit unusual optical and electronic properties,¹³ and in many ways they behave similarly to semiconductor quantum wells with the additional benefits of fabrication and integration ease. These 2D materials can be grown by simple chemical vapor deposition on a growth medium like silicon dioxide and then transferred onto a pre-existing device. This process does not require explicit lattice matching between the device and the 2D material, unlike the complicated and expensive molecular beam epitaxy process used in the growth of quantum wells. Second, unlike quantum wells, 2D materials can be easily transferred on top of a

Received: April 24, 2015

Published: July 9, 2015

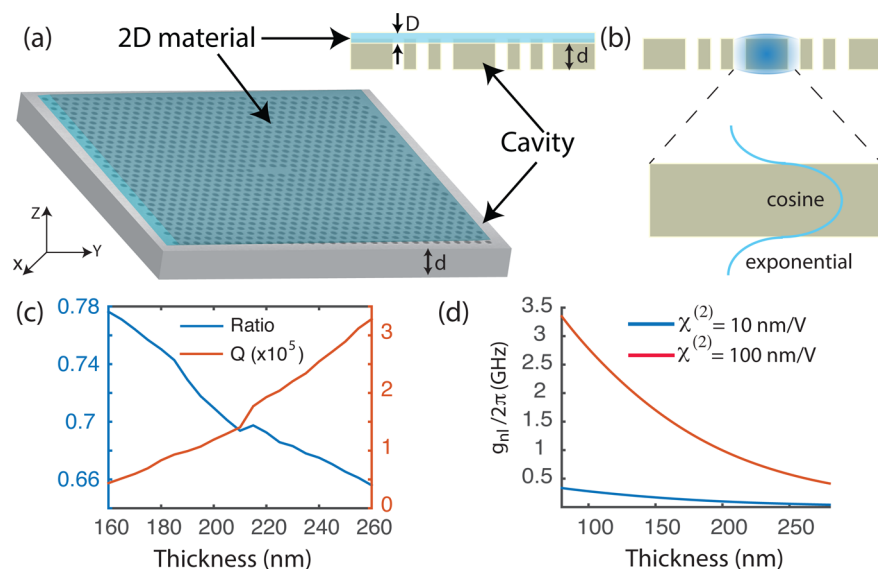


Figure 1. (a) Coupled 2D material-cavity device. A 2D material layer is transferred on top of a prefabricated cavity. The cavity thickness is d , and the 2D material thickness is assumed to be D . (b) The confined light inside the cavity can be modeled as a cosine-like function inside the slab and two exponentially decaying field profiles on the top and the bottom of the slab. (c) The ratio of the field amplitude at the surface and at the center of a generic photonic crystal cavity (silicon nitride-based nanobeam cavity) as a function of the slab thickness. The corresponding quality factor of the cavity is also plotted. The results are obtained via 3D-Finite Difference Time Domain (FDTD) simulations, for which we employed the commercial software from Lumerical Solutions. (d) The nonlinear interaction strength plotted as a function of the slab thickness.

prefabricated cavity, allowing the growth of the 2D material to be independent of the etching treatment, desirable for compatibility with modern foundry processes. Then, 2D materials could be easily restricted to a selective area by photolithography and subsequent etching, reducing unwanted losses in the device. These unique properties have generated significant interest in exploring 2D material-based nanophotonic devices,¹⁴ including electro-optic modulators,^{15,16} cavity enhanced four-wave mixing devices,¹⁷ strongly coupled 2D exciton-cavity systems,¹⁸ and optically pumped lasers.¹⁹ Despite these advances, cavity enhanced nonlinear optics with 2D materials remains largely unexplored. In this paper, we theoretically analyze a cavity integrated nonlinear 2D material device. More specifically, we focus on transition metal dichalcogenides (TMDCs). These materials demonstrate a strong off-resonant second order nonlinearity²⁰ that is notably absent in silicon or silicon nitride, the materials with current scalable fabrication methods.²¹ We provide a simple way to estimate this nonlinear strength and explore the performance of two different devices: an optically bistable device important for optical computing and a quantum optical device that can generate single photons by engineering photon–photon interactions via photon blockade.

RESULTS

Theory and Simulations. Unlike bulk materials, 2D materials interact with the cavity only via an evanescent field (Figure 1a). Hence, the maximum effective nonlinearity obtainable in a 2D material-cavity system will be smaller than with a bulk material that has the same nonlinear coefficient. The Hamiltonian \mathcal{H} describing a cavity with two modes (mode a at the fundamental and mode b at the second harmonic frequency) containing second order nonlinearity is given by¹²

$$\mathcal{H} = \Delta_a a^\dagger a + \Delta_b b^\dagger b + g_{nl} b (a^\dagger)^2 + g_{nl}^* b^\dagger (a)^2$$

Here, Δ_a and Δ_b are the detuning of the cavity modes from the laser frequency and its second-harmonic, respectively, and g_{nl} is the second-order nonlinear interaction strength, whose magnitude we want to estimate in the following. A reasonable assumption for the cavity field profile (polarized along the \hat{y} direction) confined in a high-Q photonic crystal cavity is given by a Gaussian envelope in the photonic lattice plane²² (Figure 1b)

$$\begin{aligned} \alpha_a(x, y, z) &= \alpha_b(x, y, z) \\ &= \frac{1}{\sqrt{\pi\sigma_x\sigma_y}} e^{-[(x^2/2\sigma_x^2) + (y^2/2\sigma_y^2)]} f(z) \hat{y} \end{aligned}$$

where, σ_x and σ_y are the confinement lengths of the cavity-field in the plane, and $f(z)$ is the field profile along the z -axis. The prefactor is chosen such that the normalization integral $\iiint |\alpha_a(x, y, z)|^2 dx dy dz = 1$ is satisfied, where the integration is performed over the entire volume of the cavity. We also assume that both fundamental and second-harmonic modes have only y -polarization, where the x - and y -directions are aligned to the TMDC monolayer crystal axes. Assuming a three layer model for the cavity slab, the analytic functional form of $f(z)$ reads:

$$f(z) = \begin{cases} A \cos(kz) & \text{for } |z| < d/2 \\ B e^{-k'(z-d/2)} & \text{for } |z| > d/2 \end{cases}$$

Here, A and B are the amplitudes of the field at the center and at the surface of the slab (Figure 1b). The effective nonlinearity for 2D material can be calculated from an integration performed only over the 2D material region¹²

$$\hbar g_{nl} = \epsilon_0 \left(\frac{\hbar \omega_0}{2\epsilon_0} \right)^{3/2} \sum_{ijk} \iiint dx dy dz \frac{\chi_{ijk}^{(2)}}{e^{3/2}} \alpha_{b,i} \alpha_{a,j} \alpha_{a,k}$$

where, α_{ijk} is the component of α polarized in the ijk directions, which for the calculation of the effective nonlinearity are iterated over the TMDC crystal axis directions (x,y,z) . In the case of monolayer TMDCs, which have D^{3h} symmetry, the only nonzero components of the $\chi^{(2)}$ tensor are $\chi_{yyy}^{(2)} = -\chi_{yxx}^{(2)} = -\chi_{xyx}^{(2)} = -\chi_{xyx}^{(2)}$ ²³ and therefore, the general equation for the nonlinear coupling of modes via the 2D TMDC becomes

$$\hbar g_{\text{nl}} = \varepsilon_0 \left(\frac{\hbar \omega_0}{2\varepsilon_0 \varepsilon} \right)^{3/2} \chi_{yyy}^{(2)} \iiint dx dy dz [\alpha_{b,y}(\alpha_{a,y}^2 - \alpha_{a,x}^2) - 2\alpha_{b,x}(\alpha_{a,x}\alpha_{a,y})]$$

Inputting the expressions for α_a and α_b , assumed to be purely \hat{y} polarized over the whole 2D material region, simplifies the expression to

$$\begin{aligned} \hbar g_{\text{nl}} &= \varepsilon_0 \left(\frac{\hbar \omega_0}{2\varepsilon_0 \varepsilon} \right)^{3/2} \chi_{yyy}^{(2)} \iiint dx dy dz (\alpha_{a,y}^2 \alpha_{b,y}) \\ &= \varepsilon_0 \left(\frac{\hbar \omega_0}{2\varepsilon_0} \right)^{3/2} \frac{2\chi_{yyy}^{(2)}}{3\varepsilon^{3/2} \sqrt{\pi\sigma_x\sigma_y}} \int_{z=0}^{z=D} dz B^3 e^{-3k'z} \end{aligned}$$

where ε is the dielectric constant, $\chi^{(2)}$ is the second order nonlinear coefficient of the 2D material, and D is the thickness of the 2D material. We note that a different field polarization with the same spatial pattern and total electric field strength may yield lower or even zero effective nonlinearity due to the tensor form of the nonlinear coupling. Unlike our model electric field, typical planar photonic crystal cavities (e.g., L3 or nanobeam) have nonzero field components polarized in the \hat{x} , \hat{y} , and \hat{z} directions. The contributions from the \hat{x} and \hat{y} polarizations are most significant and vary depending on the particular cavity mode. By examining the form of the nonlinear overlap we can see that when a term in the integral is antisymmetric in the x or y directions it will integrate to zero, which can be used to simplify the expression for particular modes. For TE-like polarized cavity modes in planar structures with thickness (d) less than $\lambda/2$, the \hat{z} polarized field component is very small, and it contributes only to the normalization (where it will reduce the overlap slightly).

In our analysis we have assumed that the fundamental and second harmonic modes have the same spatial profiles. Such an assumption is not strictly valid, but one needs to ensure that the integral $\iiint dx dy dz \chi^{(2)}/\varepsilon^{3/2} \alpha_a(x,y,z)^2 \alpha_b(x,y,z) \neq 0$, which amounts to the condition that one needs to satisfy phase matching. Such phase matching is difficult to realize in a nanoscale cavity,²⁴ where the integration is performed over the whole volume. For a given field pattern $\alpha_a = \alpha_{a,x}\hat{x} + \alpha_{a,y}\hat{y}$, the field pattern in mode b that maximizes the nonlinear coupling is given by $\alpha_{b,x} \propto \alpha_{a,x}\alpha_{a,y}$ and $\alpha_{b,y} \propto \alpha_{a,y}^2 - \alpha_{a,x}^2$. A mode with this exact field profile is unlikely to exist in a photonic crystal cavity, but it can be used as a guide for designing cavities (e.g., in inverse design).²⁵ However, we notice that in the case of 2D material systems the integration is performed only over the region where the material is present, giving more flexibility to the cavity design. For example, odd modes oriented normal to the surface yield almost zero mode overlap when the integration is performed over the entire cavity volume. However, due to the unique device geometry with 2D materials, the integration is performed only over one surface, and such modes are acceptable. The ability to selectively etch

the 2D material without changing the cavity parameters also opens up new possibilities for quasi-phase matching that were not possible when the cavity material is also being used as the nonlinear material. For example, in nanobeam cavity designs for second harmonic generation,²⁴ the nonlinear overlap is typically greatly reduced due to the fact that the mode is extended over several photonic crystal periods, and the field changes sign each period. When the overlap is integrated, these cancel to give very low effective nonlinearities. However, if the 2D material was etched away every other period, the overlap and, subsequently, the effective nonlinearity may be increased by orders of magnitude.

To estimate the nonlinearity, we need to estimate the magnitudes of A and B , respectively. From the continuity of the field and its derivative, we find the conditions

$$B = A \cos\left(\frac{kd}{2}\right); \quad k' = k \tan\left(\frac{kd}{2}\right)$$

The square of the field integrated over the z -axis is normalized, leading to

$$\frac{1}{A^2} = \frac{d}{2} + \frac{\sin(kd)}{2k} + \frac{\cos^2(kd/2)}{k \tan(kd/2)}$$

This can be simplified to

$$\begin{aligned} \hbar g_{\text{nl}} &= \varepsilon_0 \left(\frac{\hbar \omega_0}{2\varepsilon_0} \right)^{3/2} \frac{2\chi^{(2)}}{3\varepsilon^{3/2} \sqrt{\pi\sigma_x\sigma_y}} \frac{B^3}{3k'} (1 - e^{-3k'D}) \\ &\approx \varepsilon_0 \left(\frac{\hbar \omega_0}{2\varepsilon_0} \right)^{3/2} \frac{2\chi^{(2)} B^3 D}{3\varepsilon^{3/2} \sqrt{\pi\sigma_x\sigma_y}} \end{aligned}$$

The field amplitude B determines the strength of the field on the surface of the cavity where the 2D material is physically located. Hence, one way to increase the nonlinear interaction strength is to increase the intensity of the field at the surface, that is, by decreasing the slab thickness. Using three-dimensional Finite-Difference Time-Domain (3D-FDTD) simulations of a silicon nitride nanobeam cavity, we can determine the ratio of the electromagnetic field intensities at the surface and at the center of the cavity as a function of the cavity thickness, d . We observe a monotonic increase of the surface field with decreasing thickness (Figure 1c). However, a monotonic decrease in the Q factor is also observed with decreasing slab thickness, as with increased surface field more light can leak out. We note that this result shows only a qualitative behavior and that proper design of the cavity can improve the Q factor while maintaining comparable surface field strength. We also note that, the nonlinear interaction strength does not depend on the Q factor of the cavity, but Q is important for the low-power operation of the devices as explained below.

Next we calculate the value of the nonlinear coefficient g_{nl} for different ratios of the amplitudes of the surface and center field. Note that this ratio is the same as $B/A = \cos(kd/2)$. The analytically estimated expression for g_{nl} reveals that the interaction strength depends on the product of the second-order nonlinear coefficient $\chi^{(2)}$ and the 2D material thickness D . From previous experimental demonstrations, D is generally assumed to be the same as the interlayer distance ~ 0.65 nm, unlike the value of $\chi^{(2)}$, which can vary significantly (experimental data ranges from 0.1 to 100 nm/V for

molybdenum disulfide^{20,26,27} and 4 nm/V for tungsten disulfide²³). For our numerical investigations, we choose two representative cases: $\chi^{(2)} = 10$ and 100 nm/V, and a target wavelength of 810 nm. For the cavity, we want to use silicon compatible material to ensure scalability and compatibility with foundry processes.²¹ However, the use of silicon is prohibitive, because it is not transparent at both the fundamental and the second harmonic frequencies. As the fundamental wavelength is around 810 nm, one requires a large bandgap material, which typically corresponds to a lower refractive index. Among these materials, silicon nitride has a relatively large refractive index ($n \sim 2$). Using a photonic crystal cavity, one can reach $\sigma_x = \sigma_y = \lambda \cdot 2n$.²⁸ Figure 1d shows the nonlinear interaction strength as a function of the slab thickness, where we obtain the field ratio from the results in Figure 1c. A monotonic increase in g_{nl} is observed with decreasing d ; although, depending on the other cavity parameters, a nonmonotonic dependence on the slab thickness might be observed. This is due to the fact that, with a reduction in the thickness d , the ratio of the surface-to-center field increases. However, this reduces the center field itself due to lower confinement. These two are counteracting effects and could lead to a nonmonotonic dependence in an actual device. We note that one can enhance the interaction strength further by optimizing the cavity design to enhance the fields at the surface of the cavity without sacrificing the quality factor.

Another important consideration for cavity nonlinear optics is the loss originating from the material itself. Denoting the electric field amplitude inside the cavity as E , the mode volume of the cavity as V_m , and the relative permittivity of the cavity material as ϵ_r , we determine that the energy stored in a cavity is $E_T = \epsilon_0 \epsilon_r |E|^2 V_m$. The electric field inside the cavity (with resonant frequency ω_0 and quality factor Q) decreases with time as $E(t) = E(0) \exp(-\omega_0 t/2Q)$. If the bare cavity has a line width of $\Delta\omega_0 = \omega_0/Q$ and the integrated 2D material-cavity has a line width (due to material absorption) of $\Delta\omega$, then the energy lost due to absorption over a small time duration T is $\epsilon_0 \epsilon_r |E(0)|^2 V_m (\exp(-\Delta\omega_0 T) - \exp(-\Delta\omega T))$. The optical power absorbed in the 2D material with a conductivity of σ is given by $\sigma |E_{2D}|^2 A_m$, where E_{2D} is the electric field at the spatial location of the 2D material, and A_m is the overlap area between the cavity and the 2D material. Following previous analysis, we identify $E(0) = A$ and $E_{2D} = B$, and we can write

$$\epsilon_0 \epsilon_r |A|^2 V_m (\exp(-\Delta\omega_0 T) - \exp(-\Delta\omega T)) = \sigma |B|^2 A_m T$$

Expanding the exponential, we can simplify:

$$\Delta\omega_0 - \Delta\omega = \frac{\sigma |B|^2 A_m}{\epsilon_0 \epsilon_r |A|^2 V_m}$$

The relationship between A_m and V_m strongly depends on the cavity design, but as a rough order of magnitude, one can estimate $A_m = V_m/d$, d being the cavity thickness as explained before. For TMDCs, the conductivity σ is very close to zero at the fundamental frequency of 810 nm,²⁹ but at the second harmonic there might be significant absorption, which will limit the ultimate operation. In fact, the calculated absorptive Q is only ~ 100 . Hence, for the successful demonstration of a 2D material nonlinear device, one needs to ensure that the conductivity is close to zero at both the fundamental and the second harmonic frequencies, respectively. At a fundamental frequency of 1500 nm, this condition is satisfied, but unfortunately, the nonlinear coefficient strongly depends on frequency and is expected to decrease at longer wavelengths.

For example the reported value of $\chi^{(2)}$ for tungsten diselenide is only 0.06 nm/V at 1550 nm,³⁰ and for molybdenum disulfide, the nonlinearity peaks at around 0.85 μm , and drops significantly for pump wavelengths longer than 1 μm . With the available TMDCs, strong absorption at the second harmonic frequency poses a serious problem for operation at the frequency where the nonlinear optical effect is the strongest. Hence, the ideal wavelength of operation will be somewhere where the conductivity is lower at the second harmonic frequency and the second order nonlinear coefficient is appreciable. Current experimental measurements, however, lack such data for TMDCs. We hope that with further experimental study and exploration of new 2D materials, for example, black phosphorus^{31,32} or molybdenum ditelluride,³³ such a regime can be found.

For the following simulations, we assume $g_{nl}/2\pi = 0.2$ and 2 GHz, respectively, for a cavity thickness $d \approx 140$ nm, depending on the nonlinear interaction strength of $\chi^{(2)} = 10$ and 100 nm/V. We also assumed that the absorptive loss from the 2D material is minimal. For comparison, a similar device made out of a bulk $\chi^{(2)}$ nonlinear medium (for example, with III–V material, like GaAs with typical value of $\chi^{(2)} = 100$ pm/V), the typical nonlinear interaction strength achievable is $g_{nl}/2\pi = 1.2$ GHz.¹² Even though the effective nonlinearity in a 2D material-cavity device is not significantly higher than that of a cavity made exclusively of $\chi^{(2)}$ nonlinear material, these 2D materials offer the possibility to leverage the second order nonlinearity in a silicon compatible platform. With this analysis of the nonlinear interaction strength at hand, we can analyze the performance of nonlinear optical devices operating at low intracavity photon numbers. More specifically, we analyze two different applications: (1) an optically bistable device for all-optical switching exploiting second-order nonlinearity, and (2) single-photon blockade as a consequence of strong photon–photon repulsion, useful for prospective quantum simulation applications.

Optical Bistability. Few photon optical bistability is a necessary condition for digital optical computing. The main hurdle for this becoming a practical technology is the large optical power required to observe the bistability. One way to achieve optical bistability is through nonlinear optics, with a strong second order nonlinearity being desirable to reduce the necessary power requirements.³⁴ Proper analysis of a lossy system, such as the proposed cavity system, requires the analysis of the master equation with the addition of Lindblad terms, as outlined in ref 34. With the total cavity field decay rate through the transmission and reflections ports defined as κ , the cavity driving term becomes $E(\kappa/2)^{1/2}(a + a^\dagger)$, assuming the two ports are equivalent. The quality factor of the cavity is defined as $Q = \omega_a/2\kappa$, with ω_a being the resonance frequency of the mode a . Note that, we have assumed that the second-harmonic mode has similar Q as the fundamental mode. Such an assumption may not be valid for a realistic case, where strong absorption might occur at the second harmonic frequency, as explained earlier in the paper.

Following the formalism in ref 34, we numerically simulate the performance of the device by using the mean-field equations. Figure 2a shows clear signatures of optical bistability, both in the steady state as well as under dynamic simulation. We analyze the optical power as well as the intracavity photon number required to observe the optical bistability as a function of the cavity Q factor (Figures 2b,c). Depending on the choice of $\chi^{(2)}$, the photon number can be reduced below 100 with a

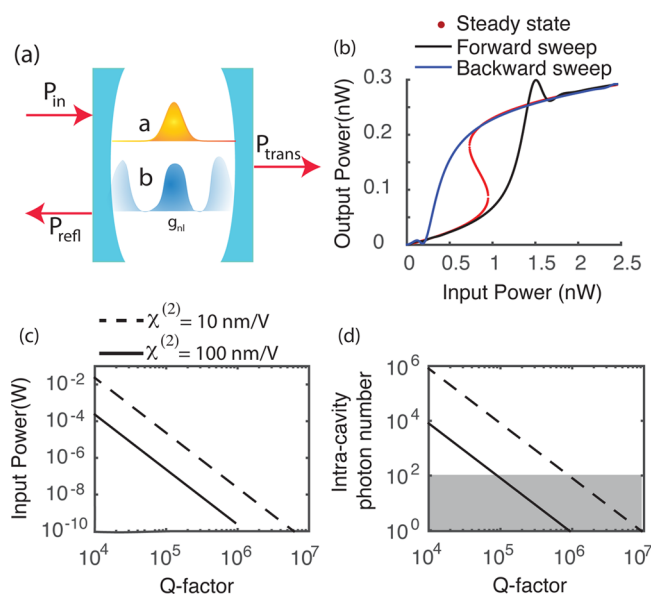


Figure 2. (a) Cavity with two modes at fundamental and second-harmonic frequencies, respectively. (b) Steady-state and dynamic bistable behavior: the steady state shows the typical bistability behavior, while the dynamic simulations show the hysteresis. (c) Required input power to observe the optical bistability as a function of the cavity quality factor for two different nonlinear coupling strengths. (d) Intra-cavity photon number as a function of the quality factor. The shaded area highlights the region where the required photon number drops below 100.

cavity Q -factor of 10^5 – 10^6 . Such quality factors can be readily achieved using silicon nitride nanobeam photonic crystal resonators.³⁵ We emphasize that this optical bistability originates from true nonlinear optical effects and differs from previous demonstrations of optical bistability based on thermo-optical nonlinearity³⁶ or photorefractive effects due to free carriers.^{37,38} With other effects, one may observe optical bistability with lower quality factor cavities, but $\chi^{(2)}$ nonlinear optical effects preserve the optical coherence, a necessary condition in the exploration of coherence in optical computing.¹ 2D material-integrated silicon nitride cavity is a promising test-bed for the exploration of such true nonlinear optical bistability. Most materials, including silicon and III–V semiconductors generate carriers through two-photon absorption, thereby leading to free carrier-based effects. However, the large band gap of silicon nitride prevents this, making silicon nitride an ideal platform to develop cavity-based optically bistable systems.

Photon Blockade. In addition to optical bistability, we also analyze the possibility of single-photon blockade, where due to the nonlinear interaction between photons, one can filter out single photons from the input laser (a coherent state). For a coherent state, the $g^{(2)}(0) = 1$, and for a perfect single photon source, $g^{(2)}(0) = 0$.³⁹ The second order autocorrelation function, $g^{(2)}(0) = \langle a^\dagger a^\dagger aa \rangle / \langle a^\dagger a \rangle^2$, is the typical figure of merit employed to probe the single photon nature of the transmitted light through a nonlinear optical cavity. A reduction in the second order autocorrelation, such as in Figure 3a, is known as photon antibunching. Note that, in the analysis of the optically bistable device, the quantum optical nature of the system is largely ignored, despite the fact that we are concerned with few photon nonlinear optics. However, to analyze the

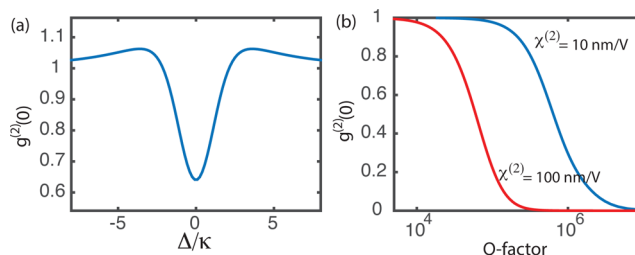


Figure 3. (a) $g^{(2)}(0)$ as a function of Δ/κ , showing a clear antibunching, and signature of photon blockade. (b) $g^{(2)}(0)$ as a function of the cavity quality factor for two different second order nonlinear interaction strengths.

photon blockade, we cannot make such simplifications and we need to perform fully quantum optical simulations.

Photon blockade has been observed in various cavity QED systems, for example, using quantum dots^{4–6} and atoms,⁷ but only very recently it has been proposed that such a purely quantum effect might be observed when bulk second¹² and third¹¹ order nonlinear materials are integrated with very high- Q cavities. Due to their centro-symmetric nature, silicon compatible materials lack a second order nonlinearity, limiting bulk silicon devices to rely on third-order nonlinear effects (unless surface effects play a major role). This greatly increases the required Q -factor to values on the order of $Q \sim 10^7$ – 10^8 for typical photonic crystal-type cavities.¹¹ With second order nonlinearity, one can utilize lower quality factor cavities, $\sim 10^5$ – 10^6 , but one would need to use a different material system that exhibits second order nonlinear susceptibility, for example, III–V materials, including GaAs or GaP. However, fabrication of even these modest quality factor cavities in these materials is often difficult, and the overall prospect of scalability is limited.

As mentioned before, 2D materials offer an interesting solution toward realizing a second order nonlinearity in a silicon compatible platform. Here we analyze whether the 2D material-cavity platform can reach the photon blockade regime. Fully quantum optical simulations are performed (with a photon basis truncated up to 10 photons), and the second order correlation $g^{(2)}(0)$ is calculated.⁴ Assuming $g_{nl}/2\pi = \kappa/2\pi = 0.2$ GHz, $g^{(2)}(0)$ of the transmitted light as a function of the laser detuning Δ from the cavity resonance shows clear antibunching ($g^{(2)}(0) < 1$) when the laser is on resonance with the cavity, indicating that a cavity enhanced 2D platform can achieve photon blockade (Figure 3a). We then studied the $g^{(2)}(0)$ as a function of the cavity quality factor (Figure 3b) at zero detuning, where the antibunching is the most prominent. A cavity quality factor of 10^5 – 10^6 is required to observe photon blockade in both the 2D material-based and III–V semiconductor-based platforms. However, the 2D material-based platform can take advantage of silicon-based cavities where nanofabrication is well developed. In fact, recent experiments have demonstrated a quality factor of ~ 55000 in silicon nitride,⁴⁰ although in theory this cavity can reach up to a quality factor of $\sim 10^6$.³⁵ To reach the regime of photon blockade with $g^{(2)}(0) \sim 0.1$, with a strongly coupled quantum dot-cavity system, one also needs a quality factor of $\sim 10^5$.⁴

Apart from quantum dots, one can in principle employ other quantum emitters based on defects. However, they generally have a lower dipole moment, leading to reduced interaction strength and, hence, require a larger quality factor. They also suffer from similar limitations to quantum dots, in terms of random positioning and inhomogeneous broadening. Another

promising approach to reach blockade is to employ nonlinear optomechanical interactions.⁴¹ Such methods provide the necessary scalability, but generally require a much larger quality factor ($\sim 10^7$ to $\sim 10^8$) assuming a mechanical resonator frequency from 100 MHz to 1 GHz. Both the quantum emitters and optomechanics-based nonlinearities are very different from the second-order nonlinearity reported here, and a direct comparison between them is difficult. However, the possibility of photon blockade clearly indicates that 2D material integrated cavities offer a solid-state alternative to quantum emitter-based systems.

CONCLUSION

The integration of two-dimensional materials with high quality factor cavities offers one potential pathway toward a scalable, silicon compatible platform for nonlinear optics. Even though the 2D material monolayer only interacts with the evanescent field of the cavity, the effective nonlinear strength is on the same order of magnitude as bulk III–V material-based cavities. Moreover, with coupling to a high Q -cavity ($\sim 10^5$ to $\sim 10^6$), the nonlinearity is comparable to the current quantum dot-based systems and is sufficiently high for demonstrations of optical bistability and photon blockade. However, this platform offers the distinct advantages of direct integration and silicon compatibility, which has been problematic to III–V based devices. Thus, this 2D-integrated platform could yield large-scale coupled cavity systems required for optics-based computing, as well as extending the fundamental study of quantum optical effects.

AUTHOR INFORMATION

Corresponding Author

*E-mail: arka@uw.edu.

Notes

The authors declare no competing financial interest.

ACKNOWLEDGMENTS

This work is supported by the National Science Foundation under Grant NSF-EFRI-1433496, and the Air Force Office of Scientific Research-Young Investigator Program under Grant FA9550-15-1-0150. The authors acknowledge useful discussions with Prof. Xiaodong Xu.

REFERENCES

- (1) Santori, C.; Pelc, J. S.; Beausoleil, R. G.; Tezak, N.; Hamerly, R.; Mabuchi, H. Quantum Noise in Large-Scale Coherent Nonlinear Photonic Circuits. *Phys. Rev. Appl.* **2014**, *1*, 054005.
- (2) Hartmann, M. J.; Brandão, F. G. S. L.; Plenio, M. B. Quantum many-body phenomena in coupled cavity arrays. *Laser Photonics Rev.* **2008**, *2*, 527–556.
- (3) Underwood, D. L.; Shanks, W. E.; Koch, J.; Houck, A. A. Low-disorder microwave cavity lattices for quantum simulation with photons. *Phys. Rev. A: At., Mol., Opt. Phys.* **2012**, *86*, 023837.
- (4) Majumdar, A.; Bajcsy, M.; Vučković, J. Probing the ladder of dressed states and nonclassical light generation in quantum-dot–cavity QED. *Phys. Rev. A: At., Mol., Opt. Phys.* **2012**, *85*, 041801.
- (5) Faraon, A.; Fushman, I.; Englund, D.; Stoltz, N.; Petroff, P.; Vuckovic, J. Coherent generation of non-classical light on a chip via photon-induced tunnelling and blockade. *Nat. Phys.* **2008**, *4*, 859–863.
- (6) Reinhard, A.; Volz, T.; Winger, M.; Badolato, A.; Hennessy, K. J.; Hu, E. L.; Imamoglu, A. Strongly correlated photons on a chip. *Nat. Photonics* **2011**, *6*, 93–96.
- (7) Birnbaum, K. M.; Boca, A.; Miller, R.; Boozer, A. D.; Northup, T. E.; Kimble, H. J. Photon blockade in an optical cavity with one trapped atom. *Nature* **2005**, *436*, 87–90.
- (8) Carusotto, I.; Ciuti, C. Quantum fluids of light. *Rev. Mod. Phys.* **2013**, *85*, 299–366.
- (9) Deng, H.; Haug, H.; Yamamoto, Y. Exciton-polariton Bose–Einstein condensation. *Rev. Mod. Phys.* **2010**, *82*, 1489–1537.
- (10) Ballarini, D.; De Giorgi, M.; Cancellieri, E.; Houdré, R.; Giacobino, E.; Cingolani, R.; Bramati, A.; Gigli, G.; Sanvitto, D. All-optical polariton transistor. *Nat. Commun.* **2013**, *4*, 1778.
- (11) Ferretti, S.; Gerace, D. Single-photon nonlinear optics with Kerr-type nanostructured materials. *Phys. Rev. B: Condens. Matter Mater. Phys.* **2012**, *85*, 033303.
- (12) Majumdar, A.; Gerace, D. Single-photon blockade in doubly resonant nanocavities with second-order nonlinearity. *Phys. Rev. B: Condens. Matter Mater. Phys.* **2013**, *87*, 235319.
- (13) Wang, Q. H.; Kalantar-Zadeh, K.; Kis, A.; Coleman, J. N.; Strano, M. S. Electronics and optoelectronics of two-dimensional transition metal dichalcogenides. *Nat. Nanotechnol.* **2012**, *7*, 699–712.
- (14) Xia, F.; Wang, H.; Xiao, D.; Dubey, M.; Ramasubramanian, A. Two-dimensional material nanophotonics. *Nat. Photonics* **2014**, *8*, 899–907.
- (15) Majumdar, A.; Kim, J.; Vuckovic, J.; Wang, F. Electrical Control of Silicon Photonic Crystal Cavity by Graphene. *Nano Lett.* **2013**, *13*, 515–518.
- (16) Gan, X.; Shiue, R.-J.; Gao, Y.; Mak, K. F.; Yao, X.; Li, L.; Szep, A.; Walker, D.; Hone, J.; Heinz, T. F.; Englund, D. High-Contrast Electrooptic Modulation of a Photonic Crystal Nanocavity by Electrical Gating of Graphene. *Nano Lett.* **2013**, *13*, 691–696.
- (17) Gu, T.; Petrone, N.; McMillan, J. F.; van der Zande, A.; Yu, M.; Lo, G. Q.; Kwong, D. L.; Hone, J.; Wong, C. W. Regenerative oscillation and four-wave mixing in graphene optoelectronics. *Nat. Photonics* **2012**, *6*, 554–559.
- (18) Liu, X.; Galfsky, T.; Sun, Z.; Xia, F.; Lin, E.-c.; Lee, Y.-H.; Kéna-Cohen, S.; Menon, V. M. Strong light–matter coupling in two-dimensional atomic crystals. *Nat. Photonics* **2014**, *9*, 30–34.
- (19) Wu, S.; Buckley, S.; Schaibley, J. R.; Feng, L.; Yan, J.; Mandrus, D. G.; Hatami, F.; Yao, W.; Vuckovic, J.; Majumdar, A.; Xu, X. Monolayer semiconductor nanocavity lasers with ultralow thresholds. *Nature* **2015**, *520*, 69–72.
- (20) Kumar, N.; Najmaei, S.; Cui, Q.; Ceballos, F.; Ajayan, P. M.; Lou, J.; Zhao, H. Second harmonic microscopy of monolayer MoS₂. *Phys. Rev. B: Condens. Matter Mater. Phys.* **2013**, *87*, 161403.
- (21) Hochberg, M.; Baehr-Jones, T. Towards fabless silicon photonics. *Nat. Photonics* **2010**, *4*, 492–494.
- (22) Akahane, Y.; Asano, T.; Song, B.-S.; Noda, S. High-Q photonic nanocavity in a two-dimensional photonic crystal. *Nature* **2003**, *425*, 944–947.
- (23) Janisch, C.; Wang, Y.; Ma, D.; Mehta, N.; Elias, A. L.; Perea-Lopez, N.; Terrones, M.; Crespi, V.; Liu, Z. Extraordinary Second Harmonic Generation in Tungsten Disulfide Monolayers. *Sci. Rep.* **2014**, *4*, 5530.
- (24) Buckley, S.; Radulski, M.; Zhang, J. L.; Petykiewicz, J.; Biermann, K.; Vuckovic, J. *Opt. Express* **2014**, *22*, 26498.
- (25) Lu, J.; Vučković, J. Nanophotonic computational design. *Opt. Express* **2013**, *21*, 13351–13367.
- (26) Malard, L. M.; Alencar, T. V.; Barboza, A. P. M.; Mak, K. F.; de Paula, A. M. Observation of intense second harmonic generation from MoS₂ atomic crystals. *Phys. Rev. B: Condens. Matter Mater. Phys.* **2013**, *87*, 201401.
- (27) Trolle, M. L.; Seifert, G.; Pedersen, T. G. Theory of excitonic second-harmonic generation in monolayer MoS₂. *Phys. Rev. B: Condens. Matter Mater. Phys.* **2014**, *89*, 235410.
- (28) Notomi, M. Manipulating light with strongly modulated photonic crystals. *Rep. Prog. Phys.* **2010**, *73*, 096501.
- (29) Li, Y.; Chernikov, A.; Zhang, X.; Rigosi, A.; Hill, H. M.; van der Zande, A. M.; Chenet, D. A.; Shih, E.-M.; Hone, J.; Heinz, T. F. Measurement of the optical dielectric function of monolayer

transition-metal dichalcogenides: MoS₂, MoSe₂, WS₂, and WSe₂. *Phys. Rev. B: Condens. Matter Mater. Phys.* **2014**, *90*, 205422.

(30) Seyler, K. L.; Schaibley, J. R.; Gong, P.; Rivera, P.; Jones, A. M.; Wu, S.; Yan, J.; Mandrus, D. G.; Yao, W.; Xu, X. Electrical control of second-harmonic generation in a WSe₂ monolayer transistor. *Nat. Nanotechnol.* **2015**, *10*, 407–411.

(31) Xia, F.; Wang, H.; Jia, Y. Rediscovering black phosphorus as an anisotropic layered material for optoelectronics and electronics. *Nat. Commun.* **2014**, *5*, 4458.

(32) Lu, S. B.; Miao, L. L.; Guo, Z. N.; Qi, X.; Zhao, C. J.; Zhang, H.; Wen, S. C.; Tang, D. Y.; Fan, D. Y. Broadband nonlinear optical response in multi-layer black phosphorus: an emerging infrared and mid-infrared optical material. *Opt. Express* **2015**, *23*, 11183–11194.

(33) Lezama, I. G.; Arora, A.; Ubaldini, A.; Barreteau, C.; Giannini, E.; Potemski, M.; Morpurgo, A. F. Indirect-to-Direct Band Gap Crossover in Few-Layer MoTe₂. *Nano Lett.* **2015**, *15*, 2336–2342.

(34) Fryett, T.; Dodson, C. M.; Majumdar, A. Cavity Enhanced Nonlinear Optics for Few Photon Optical Bistability. *Opt. Express* **2015**, *23*, 16246–16255.

(35) McCutcheon, M. W.; Loncar, M. Design of a silicon nitride photonic crystal nanocavity with a Quality factor of one million for coupling to a diamond nanocrystal. *Opt. Express* **2008**, *16*, 19136–19145.

(36) Xu, Q.; Lipson, M. Carrier-induced optical bistability in silicon ring resonators. *Opt. Lett.* **2006**, *31*, 341–343.

(37) Nozaki, K.; Tanabe, T.; Shinya, A.; Matsuo, S.; Sato, T.; Taniyama, H.; Notomi, M. Sub-femtojoule all-optical switching using a photonic-crystal nanocavity. *Nat. Photonics* **2010**, *4*, 477–483.

(38) Sodagar, M.; Miri, M.; Eftekhar, A. A.; Adibi, A. Optical bistability in a one-dimensional photonic crystal resonator using a reverse-biased pn-junction. *Opt. Express* **2015**, *23*, 2676–2685.

(39) Scully, M. O.; Zubairy, M. S. *Quantum Optics*; Cambridge University Press: Cambridge, U.K., 1997.

(40) Khan, M.; Babinec, T.; McCutcheon, M. W.; Deotare, P.; Loncar, M. Fabrication and characterization of high-quality-factor silicon nitride nanobeam cavities. *Opt. Lett.* **2011**, *36*, 421–423.

(41) Rabl, P. Photon Blockade Effect in Optomechanical Systems. *Phys. Rev. Lett.* **2011**, *107*, 063601.